SMC-TR-02-30

AEROSPACE REPORT NO.
TR-2002(8555)-8

Collisional Dephasing and the Reduction of Laser Phase-Noise to Amplitude-Noise Conversion in a Resonant Atomic Vapor

10 June 2002

Prepared by

J. G. COFFER, M. ANDERSON, and J. C. CAMPARO
Electronics and Photonics Laboratory
Laboratory Operations

Prepared for

SPACE AND MISSILE SYSTEMS CENTER
AIR FORCE SPACE COMMAND
2430 E. El Segundo Boulevard
Los Angeles Air Force Base, CA 90245

Engineering and Technology Group

THE AEROSPACE CORPORATION
El Segundo, California

REPORT DOCUMENTATION PAGE

Form Approved
OMB No. 0704-0188

1. REPORT DATE (*DD-MM-YYYY*)	2. REPORT TYPE	3. DATES COVERED *(From - To)*
10-06-2002		

4. TITLE AND SUBTITLE

Collisional Dephasing and the Reduction of Laser Phase-Noise to Amplitude-Noise Conversion in a Resonant Atomic Vapor

5a. CONTRACT NUMBER
F04701-00-C-0009

5b. GRANT NUMBER

5c. PROGRAM ELEMENT NUMBER

6. AUTHOR(S)

J. G. Coffer, M. Anderson, and J. C. Camparo

5d. PROJECT NUMBER

5e. TASK NUMBER

5f. WORK UNIT NUMBER

7. PERFORMING ORGANIZATION NAME(S) AND ADDRESS(ES)

The Aerospace Corporation
Laboratory Operations
El Segundo, CA 90245-4691

8. PERFORMING ORGANIZATION REPORT NUMBER

TR-2002(8555)-8

9. SPONSORING / MONITORING AGENCY NAME(S) AND ADDRESS(ES)

Space and Missile Systems Center
Air Force Space Command
2450 E. El Segundo Blvd.
Los Angeles Air Force Base, CA 90245

10. SPONSOR/MONITOR'S ACRONYM(S)
SMC

11. SPONSOR/MONITOR'S REPORT NUMBER(S)
SMC-TR-02-30

12. DISTRIBUTION/AVAILABILITY STATEMENT

Approved for public release; distribution unlimited.

13. SUPPLEMENTARY NOTES

14. ABSTRACT

When resonant laser light passes through a vapor, the laser's intrinsic phase fluctuations induce random variations in the atomic coherence, which, in turn, give rise to fluctuations in the medium's absorption cross section. Hence, laser phase modulation noise (PM) is converted to transmitted laser intensity (i.e., amplitude) modulation noise (AM). Here, we consider the influence of collisional dephasing on the PM-to-AM conversion process. Specifically, we measure the relative intensity noise of a diode laser beam, resonant with the Rb D_1 transition at 794.7 nm, after it has passed through a Rb^{87}/N_2 vapor as a function of nitrogen number density. Our results demonstrate that when collisional dephasing is very rapid, the spectral density of cross-section fluctuations is reduced, so that there is a significant decrease in the efficiency of PM-to-AM conversion at low Fourier frequencies. These results imply that, in general, when laser PM-to-AM conversion is the dominant noise process, pressure broadening can actually *increase* spectroscopic sensitivity.

15. SUBJECT TERMS

Phase modulation noise, Dephasing

16. SECURITY CLASSIFICATION OF:			17. LIMITATION OF ABSTRACT	18. NUMBER OF PAGES	19a. NAME OF RESPONSIBLE PERSON
				9	John Coffer
a. REPORT	b. ABSTRACT	c. THIS PAGE			19b. TELEPHONE NUMBER *(include area code)*
UNCLASSIFIED	UNCLASSIFIED	UNCLASSIFIED			(310)336-1838

Note

The material reproduced in this report originally appeared in *Physical Review A*. The TR is published to document the work for the corporate record.

Collisional dephasing and the reduction of laser phase-noise to amplitude-noise conversion in a resonant atomic vapor

J. G. Coffer,[1] M. Anderson,[1,2] and J. C. Camparo[1]
[1]*Electronics and Photonics Laboratory, The Aerospace Corporation, P.O. Box 92957, Los Angeles, California 90009*
[2]*Department of Physics & Astronomy, University of California, Irvine, California 92697-4575*
(Received 6 August 2001; published 6 February 2002)

When resonant laser light passes through a vapor, the laser's intrinsic phase fluctuations induce random variations in the atomic coherence, which in turn give rise to fluctuations in the medium's absorption cross section. Hence, laser phase modulation noise (PM) is converted to transmitted laser intensity (i.e., amplitude) modulation noise (AM). Here, we consider the influence of collisional dephasing on the PM-to-AM conversion process. Specifically, we measure the relative intensity noise of a diode laser beam, resonant with the Rb D_1 transition at 794.7 nm, after it has passed through a Rb^{87}/N_2 vapor as a function of nitrogen number density. Our results demonstrate that when collisional dephasing is very rapid, the spectral density of cross-section fluctuations is reduced, so that there is a significant decrease in the efficiency of PM-to-AM conversion at low Fourier frequencies. These results imply that, in general, when laser PM-to-AM conversion is the dominant noise process, pressure broadening can actually *increase* spectroscopic sensitivity.

DOI: 10.1103/PhysRevA.65.033807 PACS number(s): 42.50.Gy, 42.62.Fi, 42.25.Bs

I. INTRODUCTION

In the weak-field limit of radiative interactions, it is easy to think of resonant absorption as a passive process: an optical field impinges on an atom or molecule and within some cross-sectional area σ, the atom has a high probability for absorbing the radiant energy. In nearly all respects, with the exception of the field's detuning from resonance, this viewpoint considers σ as an intrinsic, static property of the medium that is independent of the field. In point of fact, however, resonant absorption is a dynamic process even in the weak-field limit. As a consequence, though a single-mode diode laser is essentially monochromatic, the field's residual stochastic variations can generate relatively large fluctuations in a resonant vapor's absorption cross section.

The consequences of field-induced cross-section fluctuations may be understood qualitatively through Beer's law [1]. If $\delta\omega(t)$ represents the stochastic frequency (i.e., phase) variations of a laser field (most typically associated with quantum noise), and $\delta E(t)$ represents the field's stochastic amplitude fluctuations (due perhaps to mode partition noise), then under the assumption that these variations are "small,"

$$\delta I(z,t)=[N]z\left(\delta\omega(t)\frac{\partial\sigma}{\partial\omega}+\delta E(t)\frac{\partial\sigma}{\partial E}\right)e^{-[N]\sigma z}. \quad (1)$$

Here, $\delta I(z,t)$ represents the random fluctuations of the light intensity transmitted to a depth z in the absorbing medium; $[N]$ is the number density of absorbing atoms or molecules in the vapor, and we note that in the case of single-mode diode lasers the phase noise term has the dominant influence. Of course, the idea of small frequency variations is problematic for a single-mode laser, since the (nearly) δ-correlated aspect of the fluctuations implies that the root-mean-square value of $\delta\omega(t)$ is exceptionally large [2]. Nonetheless, Eq. (1) makes it clear that laser phase modulation noise (PM) can be converted to transmitted intensity (i.e., amplitude) modulation noise (AM), and that the efficiency of this conversion process will depend on the density of absorbers, the magnitude of the laser's frequency fluctuations, and the sensitivity of the cross section to those fluctuations.

In the regime of high Fourier frequencies, PM-to-AM conversion finds application as a novel spectroscopic technique [3,4]. Basically, for Fourier frequencies of the field's phase fluctuations that match an atomic or molecular resonance, the absorption cross section can display large amplitude oscillations [5]. Thus, the noise spectrum of the transmitted light will show "bright lines" at resonance frequencies, yielding information on atomic structure [6] or the absorbing medium's elemental composition [7]. In the regime of low Fourier frequencies, however, (less than about 10 kHz) PM-to-AM conversion is of no utility; it is simply a source of excess noise, and as such is to be eliminated if possible. Unfortunately, as may be appreciated from Eq. (1), PM-to-AM conversion is inherent to the absorption process and cannot be eliminated [8]; it may only be ameliorated. This issue of PM-to-AM conversion is of more than academic interest, since research has shown that the performance of vapor-cell atomic clocks may be seriously limited by this noise process [9]. Though the most straightforward mitigation strategy is to simply reduce the single-mode laser's linewidth [10], and hence the level of the field's phase noise, such an option is not always viable, nor is it necessarily the optimum strategy in all situations.

To understand better how a medium's absorption cross section responds to a fluctuating field, the present study looks at the effect of collisional dephasing on the efficiency of PM-to-AM conversion. Specifically, in Secs. II and III we describe our experiment and its results examining PM-to-AM conversion in a vapor of Rb^{87} atoms perturbed by N_2 collisions. Basically, we find that there is a dramatic decrease in the efficiency of PM-to-AM conversion when the collisional dephasing rate exceeds the optical transition's Doppler-broadened linewidth. In Sec. IV, we outline a theory of PM-to-AM conversion that includes buffer-gas dephasing collisions, and we show that when the time scale of collisional dephasing is much shorter than the field's correlation

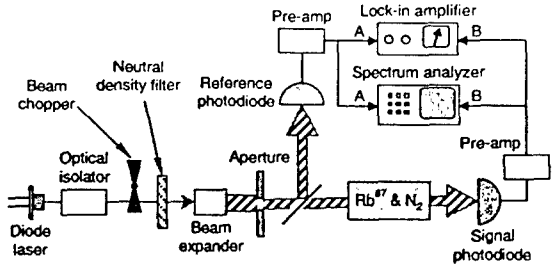

FIG. 1. Experimental arrangement as described in the text.

time, PM-to-AM conversion becomes inefficient. We conclude by considering the general spectroscopic implications of our results.

II. EXPERIMENT

According to Beer's law, fluctuations in the absorption cross section $\delta\sigma$ will manifest themselves through variations in the light intensity transmitted by a resonant vapor. Specifically, since the cross-section fluctuations we are concerned with are small

$$\langle I(z)\rangle + \delta I(z) \cong I_o e^{-[N]\langle\sigma\rangle z}(1-[N]\delta\sigma z), \qquad (2)$$

where $\langle\sigma\rangle$ is the average absorption cross section. Consequently, for a fixed number density of absorbers, the relative intensity noise or RIN (i.e., $\delta I_{\rm rms}/\langle I\rangle$) may be employed as a measure of the vapor's rms cross-section variation,

$$\delta\sigma_{\rm rms} = \frac{1}{[N]z}\frac{\delta I_{\rm rms}}{\langle I\rangle}. \qquad (3)$$

In our experiment, illustrated in Fig. 1, we examined the intensity fluctuations of a single-mode $Al_xGa_{1-x}As$ diode laser (Mitsubishi ML44126) after passing through a resonant Rb^{87} vapor contained in a Pyrex resonance cell with a N_2 buffer gas. The diode laser, emitting 5 mW and with a linewidth of 60 MHz, excited the D_1 transition of Rb at 794.7 nm, specifically, as illustrated in Fig. 2, the $5\,^2S_{1/2}(F=1)-5\,^2P_{1/2}(F'=1,2)$ transition of Rb^{87}. Due to the disparity in coupling strengths between the $F=1$ and $F'=1,2$ hyperfine levels, most of the absorption is associated with the $(F=1)$-$(F'=2)$ transition, so that to some extent the atomic system mimics a two-level atom. In the experiments, we employed several isotopically enriched Rb resonance cells with N_2 buffer-gas pressures ranging from 1 to 100 torr. The resonance cells had a diameter of 2.2 cm, a length L of 3.9 cm, and were wound with braided wire and actively stabilized to a temperature of ~38 °C (i.e., $[Rb^{87}] \cong 7.5\times10^{10}$ cm^{-3} [11]). After passing through an optical isolator, the laser beam was attenuated, expanded and then apertured so as to create a fairly uniform spatial profile. The diameter of the beam entering the resonance cell was 0.8 cm.

Prior to measuring diode laser RIN for one of our cells, we measured the number density of atoms in the absorbing $5\,^2S_{1/2}(F=1)$ state as a function of the laser intensity. Basically, we swept the diode laser frequency across the absorption line, and monitored the laser intensity with our reference

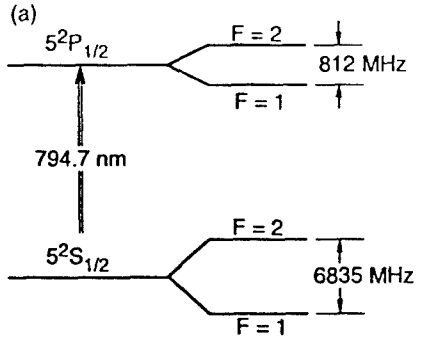

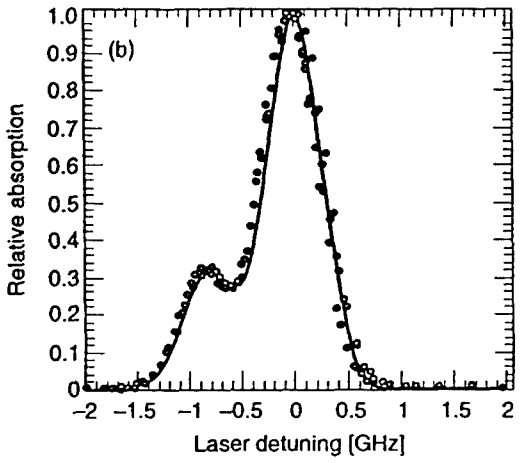

FIG. 2. (a) Relevant energy-level diagram of Rb^{87}. (b) Relative absorption features associated with the $5\,^2S_{1/2}(F=1)-5\,^2P_{1/2}$ transition in a 1-Torr N_2 cell. Zero-laser detuning corresponds to the $5\,^2S_{1/2}(F=1)-5\,^2P_{1/2}(F=2)$ transition. The solid curve is a fit to two Lorentzian functions separated by the excited-state hyperfine splitting. The resulting full width of the spectral features is 595 MHz. This is somewhat broader than the estimated Doppler width, most likely because the vapor is slightly optically thick.

and signal photodiodes. Using the reference photodiode, we could infer what the signal photodiode would have measured for the laser intensity on resonance if the Rb^{87} vapor had not been present (i.e., I_o). Then, using the on-resonance laser intensity measured with the signal photodiode $I_{\rm res}$, we determined the vapor's attenuation coefficient κ:$[Rb^{87}]\langle\sigma\rangle \equiv \kappa = 1/L\ \ln[I_o/I_{\rm res}]$. These measurements are shown in Fig. 3 for our 1-, 10-, and 100-Torr N_2 cells. For each cell, we chose an operating light intensity for the RIN measurements that was relatively large (so that shot noise on the photodetector would not confound our measurements), but small enough so that the attenuation coefficient was relatively insensitive to light-intensity variation (i.e., no optical pumping reduction of Rb^{87} [12]). For general reference, we note that at low light intensity, our average absorption cross section for the laser-tuned on resonance in the 1 torr cell was $\sim5.2\times10^{-12}$ cm^2.

The difference in the low-intensity asymptotes for the three cells is primarily due to the fact that the average absorption cross section is inversely proportional to atomic linewidth $\Delta\nu$. In the 1-Torr cell, the absorption linewidth is limited by the 510-MHz Doppler width for the D_1 transition

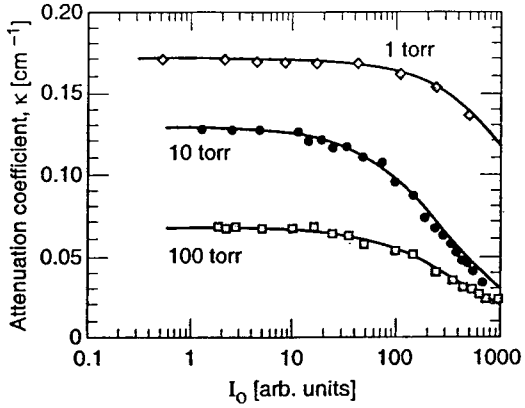

FIG. 3. Attenuation coefficient κ as a function of laser intensity. The low-intensity asymptotes differ due to the dependence of the absorption cross section on absorption linewidth.

$\Delta\nu_D$, whereas in the 100-Torr cell pressure broadening gives rise to a 1.6 GHz linewidth. (The N_2 pressure-broadening coefficient for the Rb D_1 transition is 16.3 MHz/Torr [13].) Since it was difficult to get each of the resonance cells to exactly the same temperature, the alkali number densities (and hence the $\delta\sigma_{\rm rms}$ values) were not directly comparable from cell to cell. Therefore, we used these asymptotes to calibrate our alkali densities.

As is well known, since $\Delta\nu\langle\sigma\rangle$ is essentially a constant for a given resonance [14], any variation among values of $\kappa\Delta\nu$ must be due to variations in alkali number density. Therefore, to calibrate the number density in our cells we first computed values of $\kappa_o\Delta\nu$ of each cell, where κ_o is the asymptotic value of the attenuation coefficient and $\Delta\nu \cong \sqrt{\Delta\nu_D^2+(P\beta)^2}$ [15] with P the N_2 pressure and β the N_2 pressure-broadening coefficient. We then computed the average value of $\kappa_o\Delta\nu$ for all our cells, and compared any particular cell's value of this quantity with the average. Specifically, to calibrate our measurements we multiplied the RIN by the ratio of $\kappa_o\Delta\nu$ to $\langle\kappa_o\Delta\nu\rangle$,

$$\delta\sigma_{\rm rms}=\left(\frac{\kappa_o\Delta\nu}{\langle\kappa_o\Delta\nu\rangle}\right)\frac{1}{[{\rm Rb}^{87}]L}\,\frac{\delta I_{\rm rms}}{\langle I\rangle}. \tag{4}$$

For our measurements, this procedure indicated that the average deviation of Rb^{87} among our cells was about 20%, corresponding to a cell-to-cell temperature variation of approximately ± 2°C.

Once an appropriate laser intensity was chosen for a particular resonance cell, we proceeded to the RIN measurements. First, we chopped the light and measured the average laser intensity on our reference and signal photodiodes using the lock-in amplifier. Then, without light chopping, we measured the intensity noise at ~400 Hz in a 1 Hz bandwidth with our spectrum analyzer for both the reference and signal photodiodes. Taking the ratio of the noise to average intensity gave us the laser RIN prior to entering the resonance cell and after passing through the resonant vapor. These measurements were made as a function of laser tuning Δ_o and are shown in Fig. 4 for our 1-, 10-, and 100-Torr N_2 cells. The figure shows raw RIN measurements after passing through

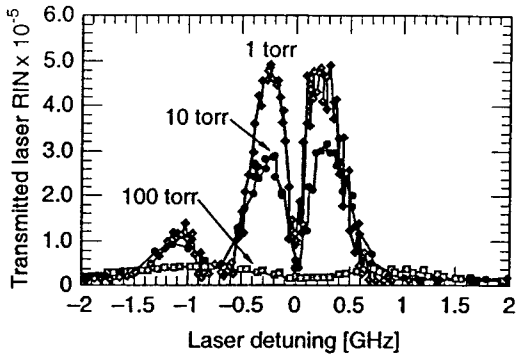

FIG. 4. Laser RIN ($\delta I_{\rm rms}/\langle I\rangle$) after passage through the resonant vapor as a function of laser detuning. Again, the zero of detuning corresponds to the $5\,^2S_{1/2}(F=1)-5\,^2P_{1/2}(F=2)$ transition. These measurements have not been corrected for cell-to-cell temperature variations, and, therefore, demonstrate that N_2 pressure has a very clear effect on PM-to-AM conversion efficiency.

the resonance cell, but *prior* to calibration for cell-to-cell temperature variations. In all cases our laser RIN before passing through the resonance cell showed no appreciable change with laser tuning [16], and on average was about 1.7×10^{-6}. Notice that except for the 100-torr resonance cell, the transmitted RIN is *nonzero* on resonance. This is in contrast to the simple interpretation of cross-section fluctuation effects expressed by Eq. (1), which indicates that the transmitted RIN is zero whenever the derivative of the absorption line shape is zero.

Figure 5 constitutes the main experimental results of the present work. There, the rms value of the cross-section fluctuations is shown as a function of the N_2 pressure, and we have calibrated the data to account for cell-to-cell temperature variations. Diamonds correspond to a laser detuning that yields a maximum in the fluctuations, while circles correspond to the laser-tuned on resonance. As the figure clearly shows, increasing the N_2 pressure beyond some critical value leads to a reduction in cross-section fluctuations.

The dashed curves correspond to fits of the data to the empirical formula

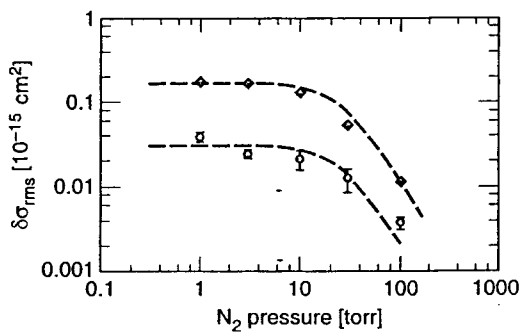

FIG. 5. Magnitude of the rms cross-section fluctuations as a function of N_2 pressure. These measurements have been corrected for cell-to-cell temperature variations as discussed in the text. Triangles correspond to the maximum value of RIN at negative detunings for each of the N_2 pressure cells, while circles correspond to on-resonance RIN. The dashed lines are fits to Eq. (5).

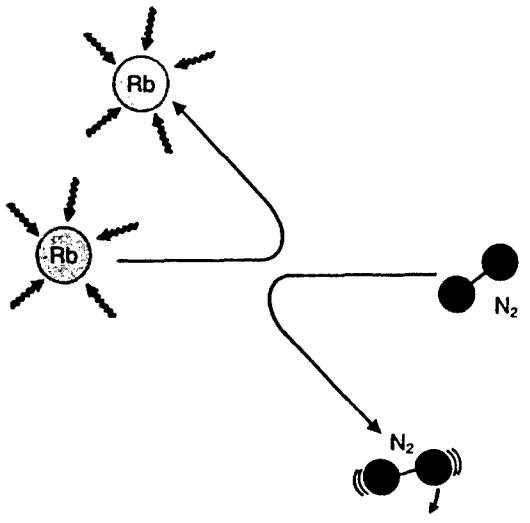

FIG. 6. Illustration of rubidium/nitrogen interaction as discussed in the text.

$$\delta\sigma_{\rm rms}=\frac{P_o^2\delta\sigma_o}{P_o^2+P^2}. \tag{5}$$

For the maximum fluctuations curve (i.e., $\Delta_o\neq 0$), $\delta\sigma_o=1.7\times10^{-16}$ cm^2, while for the on-resonance curve, $\delta\sigma_o=3.1\times10^{-17}$ cm^2. These values are clearly related to the laser's linewidth, and would be larger or smaller depending on the laser's intrinsic phase noise. For both curves, however, we obtain $P_o=27$ Torr. Thus, when the pressure-broadened linewidth is just a bit narrower than the Doppler width (i.e., $\beta P_o=440<\Delta\nu_D=510$ MHz), $\delta\sigma_{\rm rms}$ falls to about a half of its maximum value. Further, since the same value of P_o is obtained for both curves, this statement appears to be true independent of the laser tuning.

III. THEORY OF PM-TO-AM IN THE PRESENCE OF COLLISIONAL-DEPHASING

A. General considerations

Figure 6 illustrates the interaction of a Rb atom with a stochastic field and a perturbing buffer-gas molecule. We ignore three-body effects and bound-state formation, viewing the binary interaction as occurring over the time scale of a gas kinetic collision (i.e., $\tau_{\rm col}\leqslant10^{-12}$ s). For completeness, we note that kinetic and electronic energy may be transferred to the molecule during the collision, though the details of this process should have little influence on PM-to-AM conversion. Depending on the strength of the collisional perturbation, the Rb atom's interaction with the field will be altered during the encounter, and most likely "switched off" due to shifts of the atom's energy levels. Of course, the interruption of the field-atom interaction only lasts for the duration of the binary collision, and afterwards resumes. Since the mean time between Rb/buffer-gas collisions is roughly 2×10^{-10} s for a buffer gas at standard temperature and pressure, the actual time that the field-atom perturbation could be "off" is relatively small. Moreover, since the correlation time of typical laboratory fields is much longer than 10^{-12} s (i.e., $\tau_{\rm correl}\cong6\times10^{-9}$ s for a laser with a 50 MHz linewidth), the field's amplitude and frequency remain unchanged during the collision. Consequently, we can view the stochastic field as a continuous random perturbation on the atom, ignoring the collisional interruptions in this interaction.

By the same argument, however, we must recognize that the binary buffer-gas perturbation is not properly described as a continuous random process, but more akin to sudden, random impulses that scramble the phase of the field-atom interaction. Notwithstanding this recognition of the collisions' stochastic nature, we will *model* the buffer-gas perturbation as a continuous random process in what follows. This is valid, since we average atomic evolution over a time $\tau_{\rm avg}$ that is long compared to the duration of a collision but short compared to the field's correlation time (i.e., we average the collisional perturbation over $\tau_{\rm avg}$ thereby distributing its effect over this time interval).

If we restrict our attention to a two-level quantum system, then when a resonant field excites an atom or molecule the superposition it creates is just a linear combination of the ground state, $|g\rangle$, and excited state, $|e\rangle$, wave functions

$$\Phi=a_g(t)e^{-iE_gt/\hbar}|g\rangle+a_e(t)e^{-iE_et/\hbar}|e\rangle. \tag{6}$$

In this case, as may be readily shown using Maxwell's equations and the relationship between polarizability and average dipole moment [1,17], the absorption cross section has a relatively simple dependence on the expansion coefficients of Eq. (6),

$$\sigma=-\frac{16\pi^2\mu_{eg}}{\mathcal{E}_o\lambda_{eg}}{\rm Im}[a_e^*a_ge^{-i\phi(t)}]. \tag{7}$$

Here, λ_{eg} and μ_{eg} are the transition wavelength and dipole moment, respectively; $\mathcal{E}_o$ is the amplitude of the field; $\phi(t)$ is the stochastic phase of the field, and we have assumed that the index of refraction of the vapor is near unity and that the laser is tuned on resonance. (As our interest is in PM-to-AM conversion, we restrict consideration to phase-diffusion fields [18].) Written in this way, the dynamic nature of the absorption cross section is readily apparent, since variations in the expansion coefficients of the wave function will produce variations in σ.

B. Fine-grain averaged Schrödinger equation

The temporal evolution of the expansion coefficients is, of course, determined by the Schrödinger equation

$$i\hbar\frac{\partial\Phi}{\partial t}=H\Phi=(H_o+V_L+V_{\rm BG})\Phi, \tag{8}$$

where H_o is the unperturbed Hamiltonian, V_L is the perturbation due to the laser field, and $V_{\rm BG}$ is the perturbation arising from buffer-gas collisions. For the two-level atom, the laser perturbation is just

$$V_L=-\mu\frac{\mathcal{E}_oe^{i\phi(t)}}{2}e^{i\bar{\omega}t}+{\rm c.c.}, \tag{9}$$

where $\bar{\omega}$ is the average laser frequency.

With regard to the buffer gas, on a time scale that is long compared to a binary encounter, we consider that these collisions only shift the atomic state energy levels. Of course, in the case of N_2 or other molecular buffer-gas species, nonradiative relaxation of the excited state will also occur (e.g., electronic to vibrational energy transfer) [19]. However, since the optical-absorption cross section depends on the coherence between the ground and excited states, we assume that longitudinal (i.e., T_1) relaxation processes only play a secondary role in PM-to-AM conversion, with the dominant role due to transverse (i.e., T_2) relaxation processes. Thus, we write the matrix elements for the buffer-gas perturbation as

$$\langle j|V_{\mathrm{BG}}|k\rangle=\hbar\Delta_k^c(t)\delta_{jk}, \tag{10}$$

where $\Delta_k^c(t)$ is a randomly varying shift of $|k\rangle$'s energy.

Since the correlation time for these collisional energy shifts will be on the order of a gas-kinetic interaction time, $\Delta_k^c(t)$ may be considered as δ correlated. We, therefore, have $\langle\Delta_k^c\rangle=0$ and $\langle\Delta_j^c(t)\Delta_k^c(t-\tau)\rangle=\gamma_k^{\mathrm{BG}}\delta_{jk}\delta(\tau)$. Notice that if we define the random variable $\zeta(t)$ as $\Delta_g^c(t)-\Delta_e^c(t)$, then given the zero mean, δ-correlated nature of $\Delta_k^c(t)$ we have $\langle\zeta\rangle=0$ and $\langle\zeta(t)\zeta(t-\tau)\rangle=(\gamma_g^{\mathrm{BG}}+\gamma_e^{\mathrm{BG}})\delta(\tau)=\gamma_{\mathrm{BG}}\delta(\tau)$. Here, γ_{BG} is just the pressure-broadened linewidth [full width at half maximum (FWHM)] of the optical line shape.

In standard fashion [1], the coupled equations for the expansion coefficients may be obtained from Eq. (8), so that for the field tuned to resonance (i.e., $\bar{\omega}=(E_e-E_g)/\hbar$) we get

$$\dot{a}_g+ia_g\Delta_g^c(t)=\frac{i\mu_{eg}\mathcal{E}_o e^{i\phi(t)}}{2\hbar}a_e \tag{11a}$$

and

$$\dot{a}_e+ia_e\Delta_e^c(t)=\frac{i\mu_{eg}\mathcal{E}_o e^{-i\phi(t)}}{2\hbar}a_g. \tag{11b}$$

Considering the cross product of the expansion coefficients, we find from Eqs. (11) that

$$\frac{d(a_e^*a_g)}{dt}=ia_e^*a_g[\Delta_e^c(t)-\Delta_g^c(t)]-\frac{i\mu_{eg}\mathcal{E}_o e^{i\phi(t)}}{2\hbar}\times[|a_g|^2-|a_e|^2]. \tag{12}$$

Performing an ensemble average of Eq. (12) over the collisional interactions, and taking advantage of the fluctuation-dissipation theorem [20], we have

$$\left(\frac{d}{dt}+\frac{1}{2}(\gamma_{\mathrm{BG}}+A)\right)(a_e^*a_g)=-\frac{i\mu_{eg}\mathcal{E}_o e^{i\phi(t)}}{2\hbar}. \tag{13}$$

Here, we have restricted our attention to weak fields (i.e., $|a_g|^2\cong 1$ and $|a_e|^2\cong 0$), and we have included a phenomenological dephasing rate $A/2$ to account for spontaneous emission.

To proceed, we write the phase fluctuations in terms of instantaneous frequency fluctuations $\delta\omega(t)$ of the laser as

$$e^{i\phi(t)}=\exp\left[i\int_0^t\delta\omega(t')dt'\right], \tag{14}$$

where $\langle\delta\omega(t)\rangle=0$, $\langle\delta\omega(t)\delta\omega(t-\tau)\rangle=\gamma_F\delta(\tau)$, and γ_F is the linewidth of the laser field (FWHM). Then employing Eq. (14), formally solving Eq. (13), and making use of Eq. (7), we obtain

$$\sigma(t)=\frac{8\pi^2\mu_{eg}^2}{\hbar\lambda_{eg}}\mathrm{Re}\left[\int_0^t e^{-\Gamma(t-t')}\exp\left[-i\int_{t'}^t\delta\omega(y)dy\right]dt'\right], \tag{15}$$

where we have defined Γ as $\frac{1}{2}(A+\gamma_{\mathrm{BG}})$ for convenience.

C. The average cross section

To obtain the average absorption cross section, we first note that for any δ-correlated random process, $x(t)$, with $\langle x(t)\rangle=0$ and $\langle x(t)x(t-\tau)\rangle=\gamma\delta(\tau)$, we have [20]

$$\left\langle\exp\left[\pm i\int_{t'}^t x(t'')dt''\right]\right\rangle=e^{-\gamma|t-t'|/2}. \tag{16}$$

Consequently, averaging Eq. (15) over the laser fluctuations, we obtain in steady state

$$\langle\sigma\rangle=\frac{16\pi^2\mu_{eg}^2}{\hbar\lambda_{eg}}[A+\gamma_{\mathrm{BG}}+\gamma_F]^{-1}. \tag{17}$$

We note that Eq. (17) is the standard result for peak absorption cross section of a line shape, generalized here to include laser-phase fluctuations [21].

D. Estimate of the correlation time of the cross section

Given the form of Eq. (15), it seems rather obvious that the cross-section fluctuations are *not* δ-correlated, and that at a maximum the correlation time of the cross section should not be larger than Γ^{-1}. Thus, to estimate the time scale over which significant correlation exists between cross-section fluctuations, we consider $\sigma(t+\tau)$ for $\tau\ll\Gamma^{-1}$,

$$\sigma(t+\tau)=\frac{8\pi^2\mu_{eg}^2}{\hbar\lambda_{eg}}\mathrm{Re}\left[e^{-\Gamma\tau}e^{-i\phi(t+\tau)}\int_0^{t+\tau}e^{-\Gamma(t-t')}e^{i\phi(t')}dt'\right]. \tag{18}$$

Based on the δ-correlated nature of the laser frequency fluctuations, $\phi(t)$ is described as a driftless Wiener process [22], and for sufficiently small τ

$$\phi(t+\tau)=\phi(t)+\sqrt{\gamma_F\tau}N(t), \tag{19}$$

where $N(t)$ is a temporally uncorrelated, unit-normal random deviate. Using Eq. (19), and with $e^{-\Gamma\tau}\cong 1$, we have

$$\sigma(t+\tau)\cong\frac{8\pi^2\mu_{eg}^2}{\hbar\lambda_{eg}}\mathrm{Re}\left(\exp\{-iN(t)\sqrt{\gamma_F\tau}\}\times\left[e^{-i\phi(t)}\int_0^t e^{-\Gamma(t-t')}e^{i\phi(t')}dt'+\int_t^{t+\tau}\exp\{iN(t)\sqrt{\gamma_F}t\}dt\right]\right). \quad (20)$$

If τ satisfies the additional requirement that $\sqrt{\gamma_F\tau}\ll 1$, then in order of magnitude

$$[\sigma(t+\tau)-\langle\sigma\rangle]\cong\{\sigma(t)-\langle\sigma\rangle(1-\tfrac{1}{2}[A+\gamma_{BG}+\gamma_F]\tau)\}. \quad (21)$$

To the extent that the second term in brackets on the right-hand side of Eq. (21) is just $\langle\sigma\rangle$, we can say that $\sigma(t+\tau)$ and $\sigma(t)$ are correlated. We there estimate the correlation time of the cross section's fluctuations τ_c, by setting this term somewhat arbitrarily to $0.9\langle\sigma\rangle$, obtaining

$$\tau_c\cong\frac{0.2}{(A+\gamma_{BG}+\gamma_F)}. \quad (22)$$

E. Variance of the cross section

In order to evaluate the variance of the cross-section fluctuations, we first need to compute the autocorrelation function of $\sigma(t)$. From Eq. (15) we have

$$\langle\sigma^2(t)\rangle=\left[\frac{8\pi^2\mu_{eg}^2}{\hbar\lambda_{eg}}\right]^2 e^{-2\Gamma t}\left\langle\int_0^t e^{\Gamma(t_a+t_b)}\cos\left[\int_{t_a}^t\delta\omega(y)dy\right]\times\cos\left[\int_{t_b}^t\delta\omega(y)dy\right]dt_a dt_b\right\rangle \quad (23a)$$

or

$$\langle\sigma^2(t)\rangle=\frac{1}{2}\left[\frac{8\pi^2\mu_{eg}^2}{\hbar\lambda_{eg}}\right]^2 e^{-2\Gamma t}\int_0^t e^{\Gamma(t_a+t_b)}\times\left\{\left\langle\cos\left[\int_{t_a}^{t_b}\delta\omega(y)dy\right]\right\rangle+\left\langle\cos\left[2\int_{t_>}^{t}\delta\omega(y)dy+\int_{t_<}^{t_>}\delta\omega(y)dy\right]\right\rangle\right\}dt_a dt_b, \quad (23b)$$

where $t_>$ and $t_<$ refer to the greater and lesser of t_a and t_b, respectively.

Following a procedure similar to that described by Fox [20] in arriving at Eq. (16) above, it is relatively straightforward to show that

$$\left\langle\cos\left[\int_{t_a}^{t_b}\delta\omega(y)dy\right]\right\rangle=\exp[-\tfrac{1}{2}\gamma_F|t_b-t_a|] \quad (24a)$$

and

$$\left\langle\cos\left[2\int_{t_>}^{t}\delta\omega(y)dy+\int_{t_<}^{t_>}\delta\omega(y)dy\right]\right\rangle=\exp[-\tfrac{1}{2}\gamma_F(4t-3t_>-t_<)]. \quad (24b)$$

Then, using Eqs. (24a) and (24b) in Eq. (23b), and evaluating the integral, we have in steady state after some algebra

$$\langle\sigma^2\rangle=\langle\sigma\rangle^2\frac{[A+\gamma_{BG}+\gamma_F]^2}{(A+\gamma_{BG})[A+\gamma_{BG}+2\gamma_F]}. \quad (25)$$

This then yields for the variance of the cross-section fluctuations

$$\mathrm{var}[\sigma]=\langle\sigma\rangle^2\frac{\gamma_F^2}{(A+\gamma_{BG})[A+\gamma_{BG}+2\gamma_F]}. \quad (26)$$

F. Measured variance within an experimental bandwidth

For a stationary random process, it is well known that the variance is equal to the integral of the power spectral density [23]. Thus, defining $|\Sigma(f)|^2$ as the power spectral density of cross-section fluctuations at Fourier frequency f,

$$\mathrm{var}(\sigma)=\int_{-\infty}^{\infty}|\Sigma(f)|^2df. \quad (27)$$

Consequently, in order to measure the cross section's "true" variance, it is necessary to measure the fluctuations in a bandwidth much larger than τ_c^{-1}. In the present experiment, we measured the cross-section fluctuations at low Fourier frequency $f_o\cong 400$ Hz, in a 1 Hz bandwidth B.

In order to compare Eq. (26) with experiment, we approximate $|\Sigma(f)|^2$ as a constant h_o, out to τ_c^{-1}, obtaining from Eq. (27) $h_o\cong\frac{1}{2}\tau_c\mathrm{var}(\sigma)$. We then have as an estimate of the measured rms cross-section fluctuations

$$\delta\sigma_{\mathrm{rms}}=\left(\int_{f_o-B/2}^{f_o+B/2}\left|\Sigma(f)\right|^2df\right)^{1/2}\cong\sqrt{Bh_o}, \quad (28)$$

which in combination with Eqs. (22) and (26) yields

$$\delta\sigma_{\mathrm{rms}}\cong\frac{\langle\sigma\rangle\gamma_F\sqrt{0.1B}}{\sqrt{(A+\gamma_{BG})(A+\gamma_{BG}+\gamma_F)(A+\gamma_{BG}+2\gamma_F)}}=\langle\sigma\rangle\eta(\gamma_{BG},\gamma_F). \quad (29)$$

Thus, the rms cross-section fluctuations, and by Eq. (3) the laser RIN, depends on the product of the average absorption cross section and a factor η, which is related to the laser linewidth and the degree of pressure broadening.

Figure 7 shows $\delta\sigma_{\mathrm{rms}}$ as a function of nitrogen pressure P for $B=1$ Hz, $\gamma_F=60$ MHz, and $\gamma_{BG}=\beta P$ with $\beta=16.3$ MHz/Torr [13]. The two solid curves show the influence of pressure broadening on $\langle\sigma\rangle$ and η, and it is clear that the reduction of PM-to-AM conversion efficiency is due to a decrease in each of these quantities with the increasing pressure. The figure is very similar to the experimental findings, except for the fact that the falloff in PM-to-AM conversion

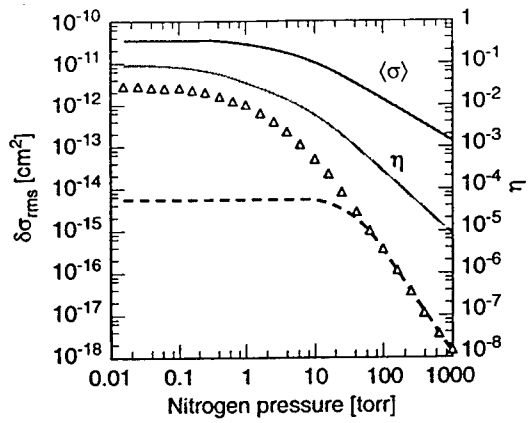

FIG. 7. Theoretical results of PM-to-AM conversion efficiency as a function of nitrogen pressure: triangles correspond to the magnitude of rms cross-section fluctuations. The two solid lines illustrate the dependence of the average cross section and the fluctuation factor η [defined by Eq. (29)], on nitrogen pressure. The dashed line is an estimate of PM-to-AM conversion efficiency when Doppler broadening is considered.

efficiency begins at much lower nitrogen pressures. This is, of course, due to the fact that we did not consider the effect of Doppler broadening in the present analysis. If we make the phenomenological substitution of $(A+\gamma_{BG}) \rightarrow \sqrt{(A+\gamma_{BG})^2+\Delta\nu_D^2}$ in Eq. (29) [15], then the dashed curve in Fig. 7 results.

For completeness, Fig. 8 shows $\delta\sigma_{rms}$ as a function of the laser linewidth for $B=1$ Hz and $P=1$ Torr N_2. Again, the two solid curves show the influence of laser linewidth on $\langle\sigma\rangle$ and η. As noted previously in the case of laser RIN [10], $\delta\sigma_{rms}$ has an extremum in its dependence on laser linewidth, which in the present analysis is seen to arise from the competing effects of $\langle\sigma\rangle$ and η on γ_F. For small laser linewidths, an increase in the laser's phase noise increases η without having much effect on $\langle\sigma\rangle$; while at larger laser linewidths, increasing laser phase noise decreases $\langle\sigma\rangle$ without affecting η.

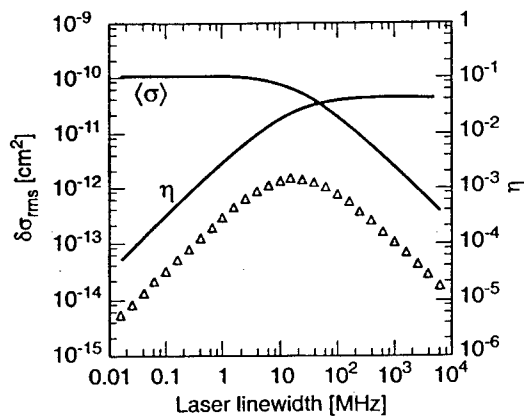

FIG. 8. Theoretical results of PM-to-AM conversion efficiency as a function of laser linewidth: triangles correspond to the magnitude of rms cross-section fluctuations. The two solid lines illustrate the dependence of the average cross section and the fluctuation factor η [defined by Eq. (29)], on laser linewidth.

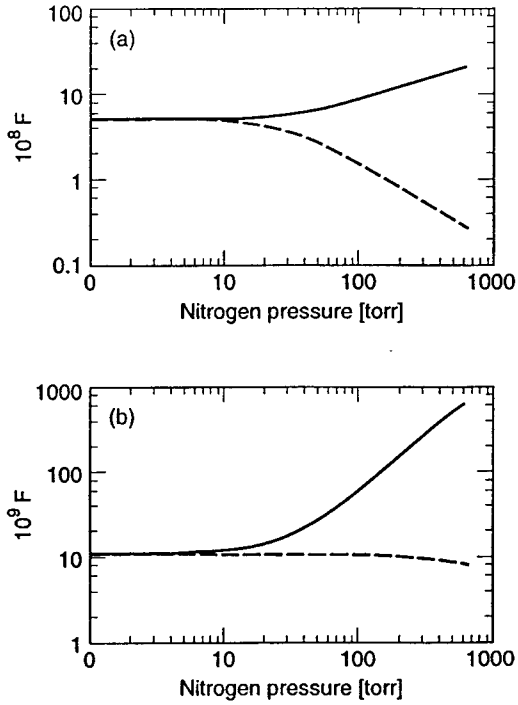

FIG. 9. (a) Spectroscopic quality factor F as a function of nitrogen pressure for a single-resonance experiment. The dashed curve is the quality factor ignoring the effect of PM-to-AM conversion on the signal-to-noise ratio. (b) Same as (a) except for the case of a double-resonance experiment.

IV. DISCUSSION

In the present work we have found both experimentally and theoretically that increasing buffer-gas pressure leads to a reduction in the efficiency of PM-to-AM conversion. This result, however, begs the question of its spectroscopic implications. The sensitivity of a spectroscopy experiment is often assessed in terms of a dimensionless quality factor F that depends on the average signal-to-noise ratio, $\langle S\rangle/N$, and the transition's linewidth relative to its center frequency, $\Delta\nu/\nu_o$,

$$F=\frac{\nu_o}{\Delta\nu}\frac{\langle S\rangle}{N}; \tag{30}$$

the larger F, the better the spectroscopic sensitivity of the experiment, all other things being equal. Typically, one considers buffer-gas pressure to have no effect on the signal-to-noise ratio and to simply increase $\Delta\nu$, thereby degrading spectroscopic sensitivity. However, as shown here, buffer-gas pressure can have a significant influence on the signal-to-noise ratio if this is limited by PM-to-AM conversion.

For a single-resonance absorption experiment, e.g., the one discussed above, the signal is just $I_o(1-\exp(-[N]\sigma L))$, and when taking advantage of lock-in techniques we are often concerned with relatively low Fourier frequencies and narrow measurement bandwidths. In such a situation, PM-to-AM conversion limits the signal-to-noise ratio in a thin vapor to $\langle\sigma\rangle/\delta\sigma_{rms}$. In combination with Eqs. (29) and (30) this yields $F=\nu_o/\eta\Delta\nu$. For illustrative purposes, Fig. 9(a) shows this quality factor as a function of

nitrogen pressure for Rb^{87} spectroscopy: $\Delta\nu = \sqrt{(A+\gamma_{BG}+\gamma_F)^2+\Delta\nu_D^2}$ and we have made the replacement of $(A+\gamma_{BG}) \rightarrow \sqrt{(A+\gamma_{BG})^2+\Delta\nu_D^2}$ in Eq. (29). For comparative purposes, the dashed line shows F as a function of N_2 pressure under the assumption that the buffer gas has no effect on the signal-to-noise ratio. As the figure clearly shows, once pressure broadening exceeds the Doppler width, the spectroscopic quality factor *increases* with the buffer-gas pressure, more than compensating for a reduction in spectroscopic sensitivity due to the increased transition linewidth. Of course, buffer-gas pressure will not increase spectroscopic resolution indefinitely, since other noise processes, most notably shot noise, will eventually come to limit the signal-to-noise ratio.

In the case of a double-resonance experiment, the linewidth of the transition may be decoupled from the PM-to-AM conversion process. For example, consider the 0-0 hyperfine transition of alkali atoms (i.e., $|F=I+\frac{1}{2}, m_F=0\rangle - |F=I-\frac{1}{2}, m_F=0\rangle$, where I is the nuclear spin), which is associated with the operation of the gas-cell atomic clock [24]. In this case, regarding Fig. 2(a) as an example, if a laser is tuned to the Rb^{87} $5\,^2S_{1/2}(F=1)-5\,^2P_{1/2}(F'=1,2)$ transition, optical pumping will create a population imbalance between the $F=2$ and $F=1$ ground-state hyperfine levels. In the absence of microwaves, transmission of the laser through a vapor is then maximized due to the reduced number of absorbers in the $F=1$ hyperfine level. However, if microwaves impinge on the vapor that are resonant with the 0-0 hyperfine transition, ν_{hfs} (6835 MHz), atoms return to the $F=1$ hyperfine level with a corresponding decrease in the transmitted light intensity. In this double-resonance situation, the signal is derived from a change in the laser absorption due to a microwave-induced number-density change, and the linewidth is associated with the hyperfine as opposed to optical transition. Again, for a thin vapor the signal-to-noise ratio is just $\langle\sigma\rangle/\delta\sigma_{rms}$. Now, however, the linewidth of the transition, $\Delta\nu_{0\text{-}0}$, is given by [25]

$$\Delta\nu_{0\text{-}0} = \sqrt{(\alpha_1 I_o + \Delta\nu_{SE} + \beta' P)^2 + (\alpha_2 P_{\mu wave})^2}, \quad (31)$$

where $\alpha_1 I_o$ is the linewidth contribution due to optical pumping [26], $\Delta\nu_{SE}$ is that due to spin exchange [27], β' is the 0-0 transition pressure-broadening coefficient, and $\alpha_2 P_{\mu wave}$ is the microwave power-broadening contribution to the linewidth [28]. (We can ignore Doppler broadening as a consequence of Dicke narrowing [29].) In the Rb atomic clock, $\alpha_1 I_o + \Delta\nu_{SE} \cong \alpha_2 P_{\mu wave} \cong 200$ Hz, and $\beta' \cong 0.3$ Hz/Torr [30]. Following the previous discussion, $F = \nu_{hfs}/\eta\Delta\nu_{0\text{-}0}$, and this quality factor is plotted in Fig. 9(b), again, the dashed line shows F as a function of N_2 pressure under the assumption that the buffer gas has no effect on the signal-to-noise ratio.

In both the single-resonance and double-resonance spectroscopic situations, we have the counterintuitive result that high buffer-gas pressure can lead to improved spectroscopic sensitivity, at least with regard to the limitations on sensitivity imposed by PM-to-AM conversion. This is especially true in the double-resonance situation, where the quality factor can easily increase by an order of magnitude. In future studies, it will be interesting to see if these spectroscopic implications prove valid, particularly in the case of double-resonance experiments, which have relevance to improving laser-pumped, gas-cell atomic clocks [31].

ACKNOWLEDGMENTS

The authors would like to thank Dr. S. Moss for many stimulating discussions during the course of these studies. This work was supported under U.S. Air Force Contract No. F040701-00-C-0009.

[1] J. I. Steinfeld, *Molecules and Radiation: An Introduction to Modern Molecular Spectroscopy* (MIT, Cambridge, 1978), Chap. 1; C. C. Davis and R. A. McFarlane, J. Quant. Spectrosc. Radiat. Transf. **18**, 151 (1977).

[2] P. Zoller and P. Lambropoulos, J. Phys. B **12**, L547 (1979).

[3] T. Yabuzaki, T. Mitsui, and U. Tanaka, Phys. Rev. Lett. **67**, 2453 (1991).

[4] R. Walser and P. Zoller, Phys. Rev. A **49**, 5067 (1994); K. V. Vasavada, G. Vemuri, and G. S. Agarwal, *ibid.* **52**, 4159 (1995).

[5] M. Bahoura and A. Clarion, Opt. Lett. **26**, 926 (2001).

[6] D. H. McIntyre, C. E. Fairchild, J. Cooper, and R. Walser, Opt. Lett. **18**, 1816 (1993); M. Rosenbluh, A. Rosenhouse-Dantsker, A. D. Wilson-Gordon, M. D. Levenson, and R. Walser, Opt. Commun. **146**, 158 (1998).

[7] R. J. McLean, P. Hannaford, C. E. Fairchild, and P. L. Dyson, Opt. Lett. **18**, 1675 (1993).

[8] J. C. Camparo, J. Opt. Soc. Am. B **15**, 1177 (1998).

[9] G. Mileti, J. Deng, F. L. Walls, D. A. Jennings, and R. E. Drullinger, IEEE J. Quantum Electron. **34**, 233 (1998); J. C. Camparo and W. F. Buell, in *Proceedings of 1997 IEEE International Frequency Control Symposium* (IEEE, Piscataway, NJ, 1997), pp. 253–258.

[10] J. C. Camparo and J. G. Coffer, Phys. Rev. A **59(1)**, 728 (1999).

[11] T. J. Killian, Phys. Rev. **27**, 578 (1926).

[12] W. Happer, Rev. Mod. Phys. **44**, 169 (1972).

[13] M. D. Rotondaro and G. P. Perram, J. Quant. Spectrosc. Radiat. Transf. **57**, 497 (1997).

[14] This result derives from the fact that the integrated absorption cross-section is a constant. See, A. C. G. Mitchell and M. W. Zemansky, *Resonance Radiation and Excited Atoms* (Cambridge University Press, London, 1971), Chap. III.

[15] C. H. Townes and A. L. Schawlow, *Microwave Spectroscopy* (Dover, New York, 1975), Chap. 13.

[16] We did notice that there was a slight variation in the laser's intrinsic RIN as we tuned the laser from −2 GHz (RIN $\sim 1.4\times10^{-6}$) to +2 GHz (RIN$\sim 2\times10^{-6}$). We attributed this to a reduction in laser RIN with increasing laser output power.

[17] A. Yariv, *Quantum Electronics* (Wiley, New York, 1989), Chap. 8.

[18] C. H. Henry, IEEE J. Quantum Electron. **QE-18**, 259 (1982);

S. F. Jacobs, Am. J. Phys. **47**, 597 (1979).
[19] L. Krause, in *The Excited State in Chemical Physics*, edited by J. Wm. McGowan (Interscience, New York, 1975), Vol. XXVIII, Chap. 4.
[20] R. F. Fox, J. Math. Phys. **13**, 1196 (1972).
[21] R. C. Hilborn, Am. J. Phys. **50**, 982 (1982); **51**, 471(E) (1983).
[22] D. T. Gillespie, Am. J. Phys. **64**, 225 (1996).
[23] R. B. Blackman and J. W. Tukey, *The Measurement of Power Spectra* (Dover, New York, 1959).
[24] J. C. Camparo and R. P. Frueholz, J. Appl. Phys. **59**, 301 (1986).
[25] J. C. Camparo and R. P. Frueholz, Phys. Rev. A **31**, 1440 (1985).
[26] J. Vanier, Can. J. Phys. **47**, 1461 (1969).
[27] J. Vanier, C. Jacques, and C. Audoin, Phys. Rev. A **31**, 3967 (1985).
[28] J. C. Camparo, Phys. Rev. A **39**, 69 (1989).
[29] R. H. Dicke, Phys. Rev. **89**, 472 (1953); R. P. Frueholz and C. H. Volk, J. Phys. B **18**, 4055 (1985).
[30] We assume that the Rb^{87} 0-0 hyperfine transition dephasing rate associated with N_2 buffer-gas collisions is roughly equal to that of Rb^{85}. See, J. Vanier, J.-F. Simard, and J.-S. Boulanger, Phys. Rev. A **9**, 1031 (1974).
[31] Y. Ohuchi, H. Suga, M. Fujita, T. Suzuki, M. Uchino, K. Takahei, M. Tsuda, and Y. Saburi, in *Proceedings of the 2000 IEEE/EIA International Frequency Control Symposium & Exhibition* (IEEE, Piscataway, NJ, 2000), pp. 651–655.

LABORATORY OPERATIONS

The Aerospace Corporation functions as an "architect-engineer" for national security programs, specializing in advanced military space systems. The Corporation's Laboratory Operations supports the effective and timely development and operation of national security systems through scientific research and the application of advanced technology. Vital to the success of the Corporation is the technical staff's wide-ranging expertise and its ability to stay abreast of new technological developments and program support issues associated with rapidly evolving space systems. Contributing capabilities are provided by these individual organizations:

Electronics and Photonics Laboratory: Microelectronics, VLSI reliability, failure analysis, solid-state device physics, compound semiconductors, radiation effects, infrared and CCD detector devices, data storage and display technologies; lasers and electro-optics, solid state laser design, micro-optics, optical communications, and fiber optic sensors; atomic frequency standards, applied laser spectroscopy, laser chemistry, atmospheric propagation and beam control, LIDAR/LADAR remote sensing; solar cell and array testing and evaluation, battery electrochemistry, battery testing and evaluation.

Space Materials Laboratory: Evaluation and characterizations of new materials and processing techniques: metals, alloys, ceramics, polymers, thin films, and composites; development of advanced deposition processes; nondestructive evaluation, component failure analysis and reliability; structural mechanics, fracture mechanics, and stress corrosion; analysis and evaluation of materials at cryogenic and elevated temperatures; launch vehicle fluid mechanics, heat transfer and flight dynamics; aerothermodynamics; chemical and electric propulsion; environmental chemistry; combustion processes; space environment effects on materials, hardening and vulnerability assessment; contamination, thermal and structural control; lubrication and surface phenomena.

Space Science Applications Laboratory: Magnetospheric, auroral and cosmic ray physics, wave-particle interactions, magnetospheric plasma waves; atmospheric and ionospheric physics, density and composition of the upper atmosphere, remote sensing using atmospheric radiation; solar physics, infrared astronomy, infrared signature analysis; infrared surveillance, imaging, remote sensing, and hyperspectral imaging; effects of solar activity, magnetic storms and nuclear explosions on the Earth's atmosphere, ionosphere and magnetosphere; effects of electromagnetic and particulate radiations on space systems; space instrumentation, design fabrication and test; environmental chemistry, trace detection; atmospheric chemical reactions, atmospheric optics, light scattering, state-specific chemical reactions and radiative signatures of missile plumes.

Center for Microtechnology: Microelectromechanical systems (MEMS) for space applications; assessment of microtechnology space applications; laser micromachining; laser-surface physical and chemical interactions; micropropulsion; micro- and nanosatellite mission analysis; intelligent microinstruments for monitoring space and launch system environments.

Office of Spectral Applications: Multispectral and hyperspectral sensor development; data analysis and algorithm development; applications of multispectral and hyperspectral imagery to defense, civil space, commercial, and environmental missions.